



## THE EFFECT OF AXIAL LOAD ON PROGRESSION OF OUT-OF-PLANE INSTABILITY IN RECTANGULAR RC WALLS

F. Dashti<sup>(1)</sup>, M. Tripathi<sup>(2)</sup>, RP. Dhakal<sup>(3)</sup>, S. Pampanin<sup>(4)</sup>

<sup>(1)</sup> Research Associate, Quake Centre, University of Canterbury, New Zealand, [farhad.dashti@canterbury.ac.nz](mailto:farhad.dashti@canterbury.ac.nz)

<sup>(2)</sup> Research Associate, Quake Centre, University of Canterbury, New Zealand, [mayank.tripathi@canterbury.ac.nz](mailto:mayank.tripathi@canterbury.ac.nz)

<sup>(3)</sup> Professor, Department of Civil and Natural Resources Engineering, University of Canterbury, New Zealand, [rajesh.dhakal@canterbury.ac.nz](mailto:rajesh.dhakal@canterbury.ac.nz)

<sup>(4)</sup> Professor, Department of Structural and Geotechnical Engineering, Sapienza University of Rome, Italy, [stefano.pampanin@uniroma1.it](mailto:stefano.pampanin@uniroma1.it)

### Abstract

Axial load is considered as a parameter in the New Zealand concrete design standard (NZS3101:2006) for prevention of out-of-plane instability in structural walls, and the minimum thickness requirement to safeguard against this mode of failure is applicable for walls with axial load ratios greater than 0.05. This study investigates the effect of axial load on development of out-of-plane instability in rectangular walls. For this purpose, the in-plane and out-of-plane responses of two rectangular wall specimens designed according to NZS3101:2006 are presented. The specimens were subjected to different axial load ratios in addition to the lateral cyclic load and the corresponding bending moment, representing a shear-span ratio of 3.0, and their out-of-plane displacement was measured using the string potentiometers mounted along the height of the boundary zones. The effects of axial load on initiation and progression of out-of-plane displacement as well as on variation of strain gradients along the length and height of the specimens and at different stages of the applied cyclic loading are studied. The point in the drift history corresponding to the maximum out-of-plane displacement proved to depend on the level of axial load. With higher axial loads, this point would shift towards the beginning of reloading in the opposite direction and the out-of-plane displacement could recover faster due to faster development of crack closure. The axial load affects the level of strain developed in the longitudinal reinforcement at different stages of a loading cycle. Although its effect on the maximum tensile and compressive strains is negligible, the strain history between these two extremes is significantly controlled by the variation of this parameter. Therefore, the axial load can prevent development of high residual strains in the reinforcement and contribute to crack closure to happen before any out-of-plane deformation can initiate. However, if this crack closure does not happen on time, the axial load can trigger faster development of out-of-plane deformation by increasing the P-delta effect.

*Keywords: Reinforced Concrete, Structural Walls, Axial Load, Out-of-plane Instability*



## 1. Introduction

According to the observations of the recent earthquakes in Chile and New Zealand, out-of-plane (OOP) instability of RC walls was one of the failure patterns that raised concerns about performance of buildings designed using modern codes [1]. Prior to the Chile earthquake, this failure mechanism had only been primarily observed in laboratory tests [2-4]. OOP instability refers to the buckling of a portion of a wall section out-of-plane, as a result of in-plane cyclic loading as a result of inelastic flexural response during an earthquake. This mode of failure is typically limited to an end region of the wall where vertical tension and compression strains from in-plane cyclic flexure are greatest [5]. Analytical [6, 7], numerical [8, 9] and experimental [10-12] investigations have been conducted to study this failure mechanism as well as its controlling parameters. Both singly reinforced and doubly reinforced concrete walls have been studied under uni-directional and bi-directional loading. A simplified approach making use of concrete columns representing boundary zones of rectangular walls has also been used to reduce the computational and experimental costs of the research programs [3, 13-16]. Based on the numerical and experimental parametric studies [17-19], the controlling parameters were classified into: i) slenderness (unsupported height-to-thickness) ratio; ii) the parameters that govern the vertical strain history and vertical strain gradients (e.g. axial load, wall length, longitudinal reinforcement ratio, concrete strength, loading history, etc.) and iii) OOP boundary conditions and different sources of eccentricity. Axial load is considered as a parameter in the New Zealand concrete design standard (NZS3101:2006 [20]) for prevention of out-of-plane instability in structural walls, and the minimum thickness requirement to safeguard against this mode of failure is applicable for walls with axial load ratios greater than 0.05. This is while global out-of-plane instability was observed in one the rectangular wall specimens tested in the literature (Specimen R2 [2]), which was not subjected to any axial load. This paper summarizes the salient features regarding the effects of axial load on progression of OOP instability in rectangular walls. The results of an experimental study on the effects of this parameter are presented, and the key observations are discussed. Moreover, the in-plane and OOP responses of the tested specimens are numerically simulated and compared with the experimental measurements.

## 2. Test program

The test specimens were designed according to New Zealand concrete design standard (NZS3101 2006 [21]). The thickness of the specimens was determined to be slightly higher than the minimum thickness requirement of the code to safeguard against OOP instability. The minimum thickness requirement calculated according to Equation 11-20 of the standard was 223 mm and the thickness of the prototype wall was determined as 250 mm. Based on the laboratory restrictions on loading and geometry, the test specimens was decided to be half-scale (1:2) model, representing the first story of a multi-storey high wall and had a shear span of 6.0 m. The unsupported height of the specimen was 2.0 m; thereby representing a storey height of 4.0 m. The general characteristics of the specimens are summarized in Table 1. The main features of the test setup and the instrumentation, whose measurements are used in this study, are displayed in Fig. 1. Further details on properties of the specimens can be found in Dashti et al [22].

## 3. Response of the specimens

Specimen RWB was tested in 2015. However, due to the structural laboratory decanting and refurbishment process, the test of Specimen RWA had to be postponed until 2018. Test observations, with focus on the significant stages of the measured response, crack patterns as well as failure modes of Specimens RWB are comprehensively reported in Dashti [23] and Dashti et al [22]. The key milestones and failure pattern of the specimens are summarized in Table 2. Specimen RWA was a replica of Specimen RWB (the benchmark specimen) in terms of dimensions and reinforcement configuration but was subjected to a smaller axial load ( $0.02f_c A_g$ ). Similar to Specimen RWB, this specimen responded predominately in flexure and started to exhibit OOP deformation during the first 1.5% drift cycle. Progression of bar fracture and bar buckling was



observed during the 2.0% drift cycles followed by accelerated concrete crushing and development of localized OOP instability during the first 2.5% drift cycle.

Table 1. General characteristics of the test specimens and the cyclic loading protocol

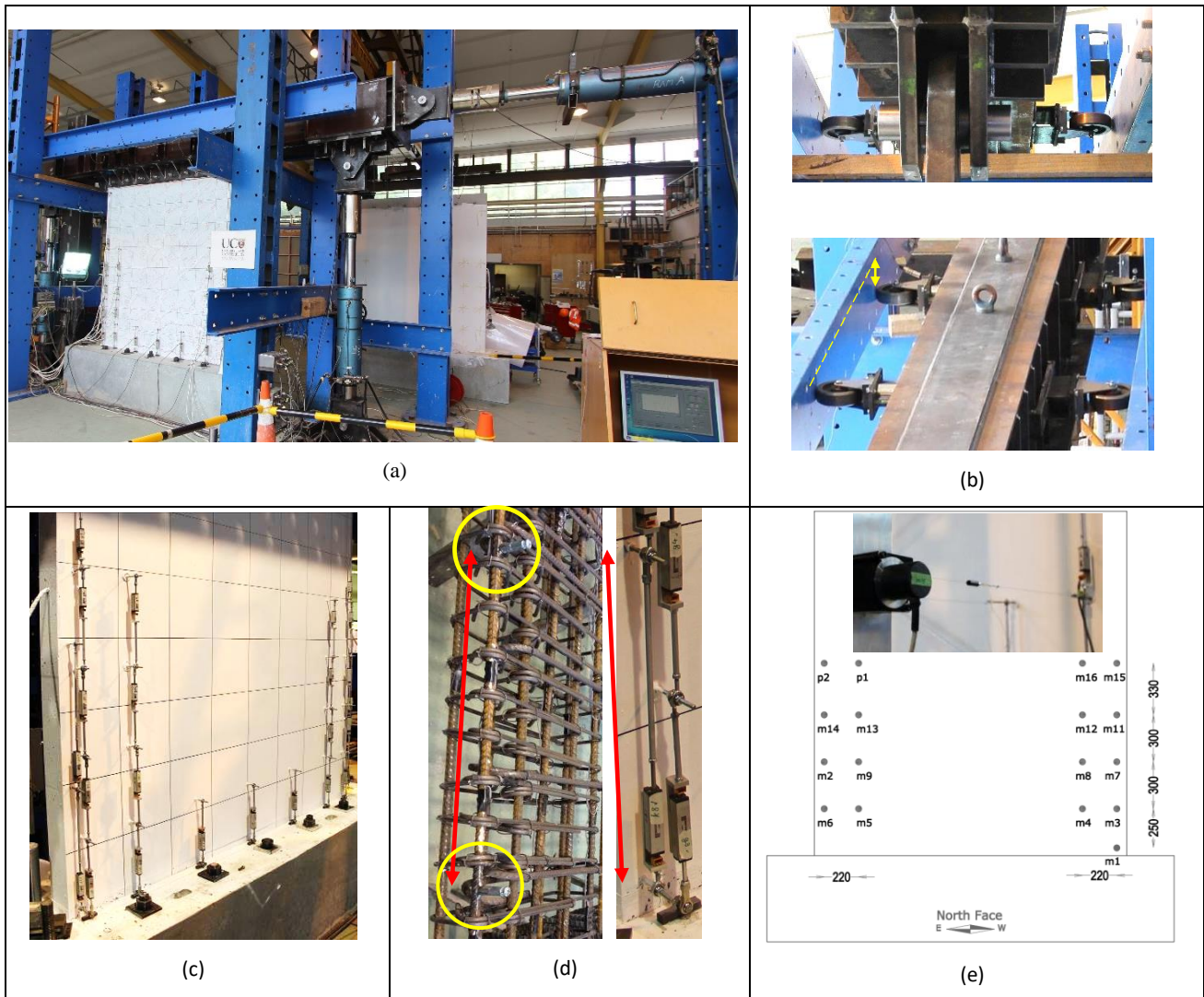
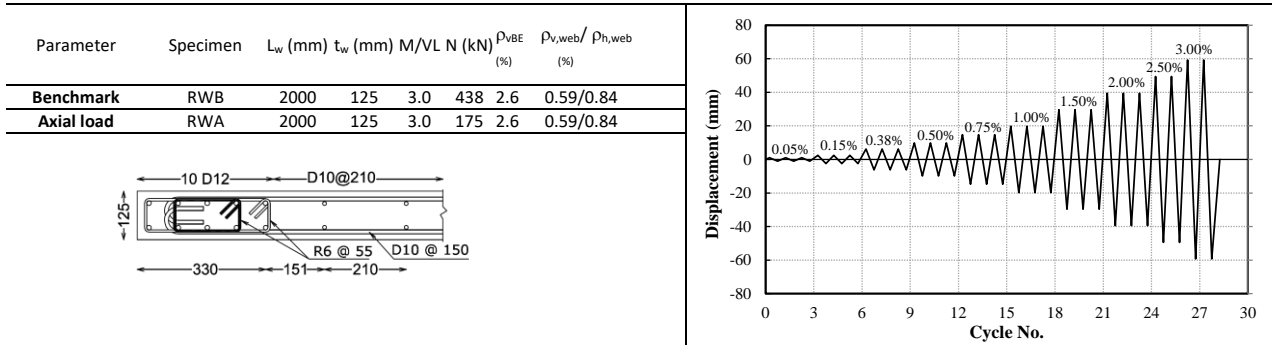


Fig. 1. Test setup: (a) configuration of the actuators; (b) OOP support; (c) linear potentiometers-north face; (d) strain gauges, welded couplers and linear potentiometer attached to the couplers for measuring the average reinforcement strain; (e) string potentiometer for measurement of OOP displacement



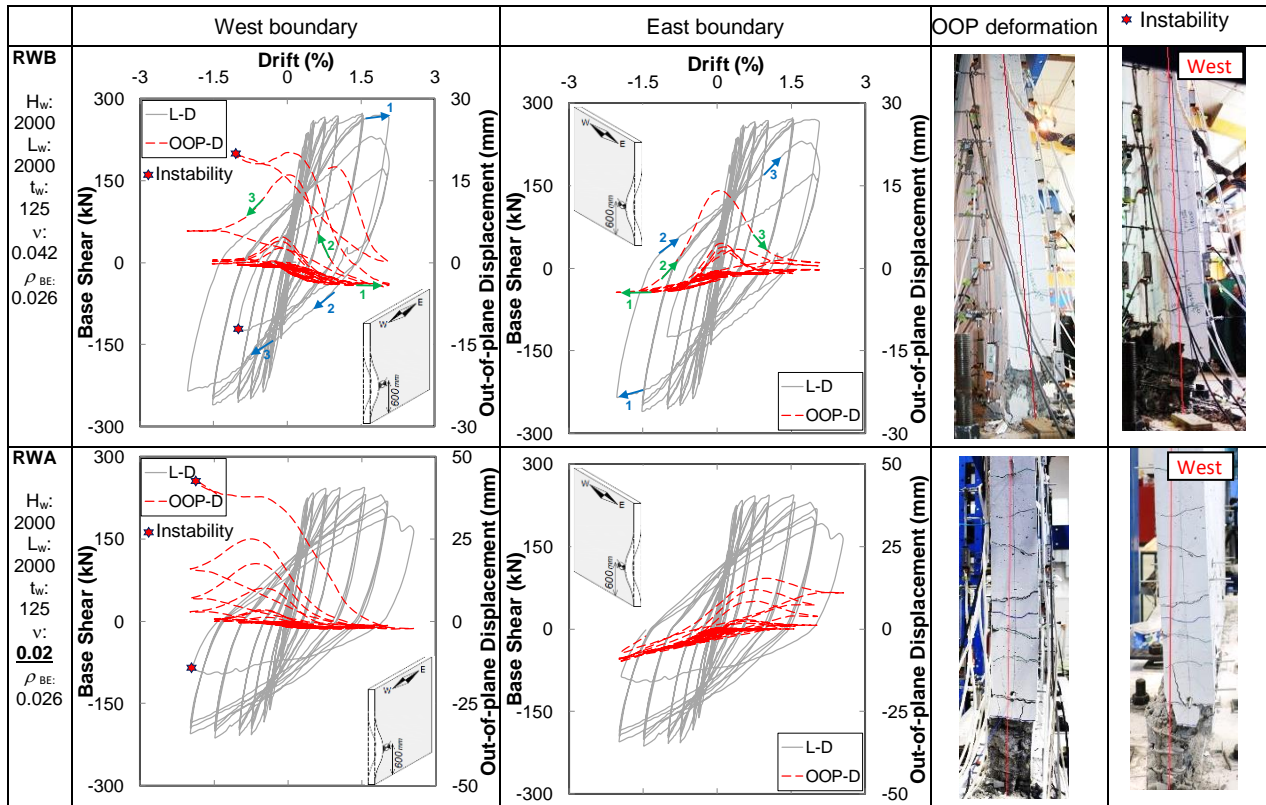
Table 2. Drift levels corresponding to key stages of wall response

Specimen	Crack initiation	Yielding	Cover spalling	Initiation of OOP deformation	Bar fracture	Bar buckling	Concrete crushing	Local OOP instability (secondary failure)
RWB	0.05% (1 <sup>st</sup> cycle)	0.5% (1 <sup>st</sup> cycle)	1.0% (1 <sup>st</sup> cycle)	1.5% (1 <sup>st</sup> cycle)	2.0% (1 <sup>st</sup> and 2 <sup>nd</sup> cycles)	2.0% (1 <sup>st</sup> and 2 <sup>nd</sup> cycles)	2.0% (2 <sup>nd</sup> cycle)	2.0% (2 <sup>nd</sup> cycle)
RWA	0.05% (1 <sup>st</sup> cycle)	0.5% (1 <sup>st</sup> cycle)	1.0% (1 <sup>st</sup> cycle)	1.5% (1 <sup>st</sup> cycle)	2.0% (1 <sup>st</sup> , 2 <sup>nd</sup> and 3 <sup>rd</sup> cycles)	2.0% (1 <sup>st</sup> , 2 <sup>nd</sup> and 3 <sup>rd</sup> cycles)	2.0% (3 <sup>rd</sup> cycle)	2.5% (1 <sup>st</sup> cycle)

The evolution of the OOP displacements in the boundary zones of the tested specimens at the elevation of 600 mm from the base, where the maximum OOP displacement was measured, is presented in Fig. 2. The lateral load versus top displacement response (L-D) of the specimens is plotted along with the OOP displacement versus top displacement (OOP-D) measurement for both boundary zones. The initial visually observed OOP deformation and the instability mode are also indicated in this figure. The stages of development of OOP deformation during one of the ultimate cycles of RWB are demonstrated using arrows that show the direction of loading and the corresponding OOP response for each boundary zone. Stage 1 represents the peak displacement level during the applied drift cycle which imposes high tensile strains to the boundary zone and generates wide flexural cracks along the boundary region. During unloading and reloading of the specimen in the opposite direction, the reliance of compressive load carrying capacity of the section solely on the reinforcement results in the development of compressive yielding in the bars while the cracks are still open, resulting in progression of OOP deformation in the boundary region. This initiation of OOP deformation is denoted as Stage 2. When the cracks start to close on the concave face of the OOP deformation profile, thereby re-engaging the contribution of concrete to the load-carrying capacity of the section, the OOP deformation starts to recover (demonstrated as Stage 3). These stages of progression and recovery of OOP deformation are numerically and experimentally investigated by the authors in previous studies [9, 12].

The OOP deformation initiated during the 1.5% drift cycles in both specimens. However, progression of this mode of deformation was followed by bar fracture and bar buckling during the 2.0% drift cycles. Both specimens exhibited local instability due to a combination of the OOP deformation and asymmetry of the cross section at the base created by the uneven failure of the reinforcement followed by irregular concrete crushing. This mode of instability is different from the global OOP instability. The difference between these two types of instability are discussed by Dashti et al [24, 25]. The boundary zones where the instability was observed in each specimen are shown in Fig. 2. The OOP deformation history of the failed boundary zone in each specimen exhibits irrecoverable and steadily increasing of OOP displacement at the onset of instability. The maximum OOP displacement was localized at the base of the specimens, where the stability of the section was impaired by the failure of the longitudinal reinforcement and concrete. The stage of instability shown in the OOP deformation history of the boundary regions is associated with the excursion of maximum force at the compression toe of the specimens.

The level of reinforcement strain at different stages of loading, unloading and reloading has been identified as one of the key parameters controlling the OOP deformations of rectangular walls. As the strain gauges exceeded their limited range of functionality before reaching this stage, the average strains of the end region bars calculated using measurements of the linear potentiometers that were welded to these bars are plotted against the top displacement of the specimens in Fig. 3. The strain histories shown in this figure correspond to gauge lengths of 447 and 445 mm for RWB and RWT, respectively, spanning the height starting from 75 mm from the base of the specimens. As the OOP deformation started during the 1.5% drift cycles in both specimens, the strain histories are plotted up to the 3<sup>rd</sup> 1.5% drift cycle to study the correlation between this parameter and the OOP response. The corresponding OOP displacement histories measured at the elevation of 600 mm from the base of the specimens are also plotted in Fig. 3.



H<sub>w</sub>: Unsupported height; L<sub>w</sub>: Length; t<sub>w</sub>: Thickness; v: Axial load ratio [N/(f<sub>c</sub>A<sub>c</sub>)]; ρ<sub>BE</sub>: Longitudinal reinforcement ratio of the boundary regions;

Fig. 2. In-plane and OOP response of the tested specimens

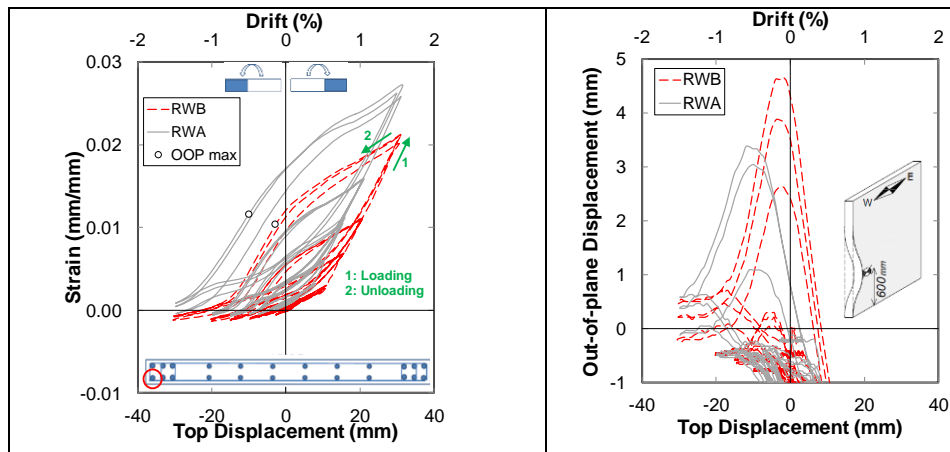


Fig. 3. Strain history of the boundary region reinforcement and evolution of OOP deformation in the west boundary region

As it can be seen in Fig. 3, strain history of the specimen with a lower axial load (RWA) was different from that of RWB both in terms of the strain values and the slope of the curve particularly in the negative drift region. The delay in flattening of the curve indicates the delay of crack closure which results in consequent delays of the maximum OOP displacement point and the OOP recovery initiation point (measured at -0.5% drift) in this specimen compared to RWB (measured at -0.2% drift). It should be noted that the maximum OOP displacement corresponds to the initiation of crack closure on the concave face of the OOP deformation profile at the elevation of maximum OOP displacement. Since the potentiometer used



for this strain comparison covered a lower elevation in both specimens, the value of strain corresponding to the maximum OOP displacement is not zero in these curves.

The strain gradients along the length and height of the specimens at the stages of peak displacement (denoted as “1”), initiation of OOP deformation (denoted as “2”) and maximum OOP deformation (denoted as “3”) are shown in Fig. 4 and Fig. 5, respectively. The values of OOP displacement in different specimens corresponding to these strains are relatively close, with the maximum OOP displacement in the range of 2-3 mm. The OOP displacement profiles are also indicated along with the strain gradients along the height of the specimens. The nonlinearity of the strain gradients along the length of the specimens at different stages of formation and recovery of OOP deformation can be seen in Fig. 4. This nonlinearity shows that the bars along a significant length of the west region of the wall have yielded in compression due to the strain travel from Stage 1 to Stage 3 and at the 300 mm spacing from the base. The nonlinearity of strain gradients in structural walls is discussed by Dashti et al [26]. The strain state at Stage 3 of both specimens indicates progression of crack opening on the east side of the specimens while the previously formed cracks of the west region are still wide open. Development of yielding in compression along the length of the wall prior to crack closure does clearly contribute to stiffness degradation of the wall against OOP deformation. Fig. 4 also shows the effect of axial load on the strain distribution at the wall base. The decrease of axial load resulted in lower compressive strains and reduction of the neutral axis depth.

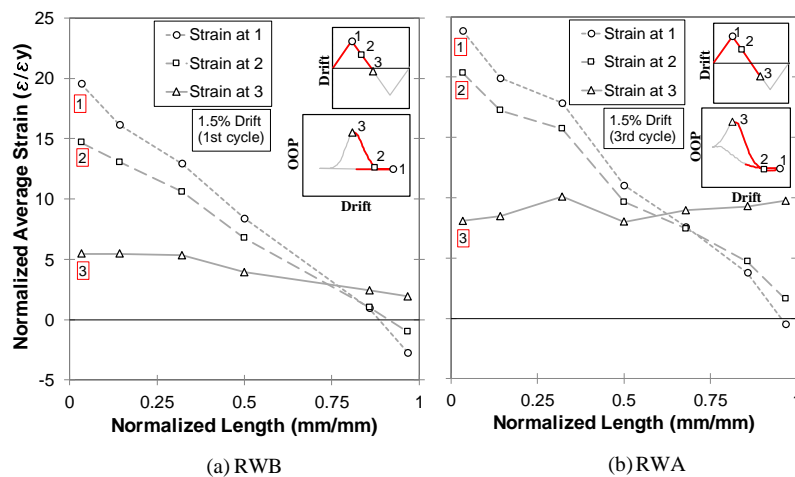


Fig. 4. Strain distribution along the length of the specimens at: (1) peak displacement level; (2) onset of OOP deformation; (3) onset of OOP recovery

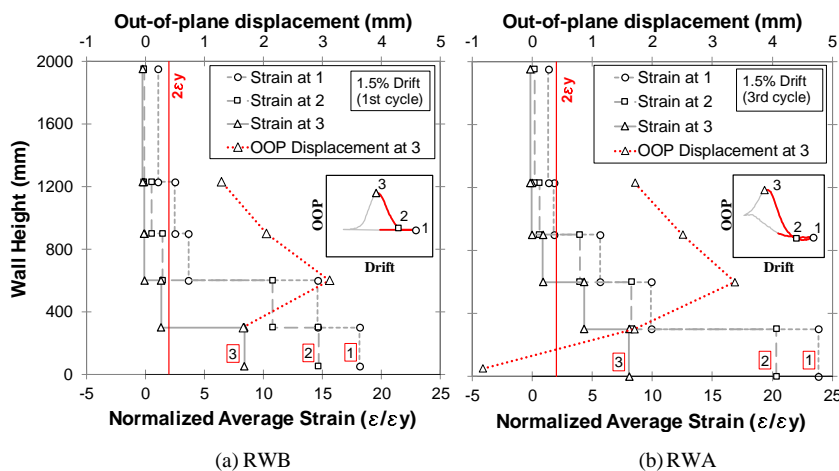


Fig. 5. Strain distribution along the height of the boundary region at: (1) peak displacement level; (2) onset of OOP deformation; (3) onset of OOP recovery



### 4. FEM Predictions vs Experimental Measurements

A numerical modelling approach based on the curved shell finite element was proposed to predict out-of-plane instability of rectangular structural walls under pure in-plane loading [8]. The modelling approach was comprehensively validated against results of several tested wall specimens [27, 9, 17] and was used to investigate the effects of different parameters on development of this mode of failure in doubly reinforced rectangular walls [18]. This numerical model is used in this section to simulate the in-plane and OOP responses of the tested specimens. Fig. 6 compares the numerical lateral load versus top displacement response and OOP displacement versus top displacement response of the specimens with the experimental measurements. The numerical response is indicated for two different step sizes of 2 mm and 0.5 mm. As can be seen in this figure, the OOP predicted by the model with the 2 mm step size initiated at higher drift levels compared to the test results, albeit with relatively large initial OOP displacement values. The analysis step size is therefore reduced to 0.5 mm in this section to investigate the effect of the step size on accuracy of the prediction. The numerically predicted OOP response histories of the specimens are within acceptable ranges in terms of the overall trend of initiation, increase and recovery of the OOP deformation and the cyclic loading stages corresponding to these steps of OOP response. The reasonably accurate prediction of the effect of axial load on the migration of the maximum OOP displacement of the west boundary region from zero drift region towards the negative top displacement region is a good case in point. The comparison of the OOP displacement histories predicted using these two step sizes indicate the sensitivity of the response to the step size and better prediction of the initial OOP displacement using smaller step size. The drift level corresponding to the onset of the OOP deformation is therefore overestimated when a large step size is used and the abrupt development of a large OOP displacement could be an indication of the rather large step size.

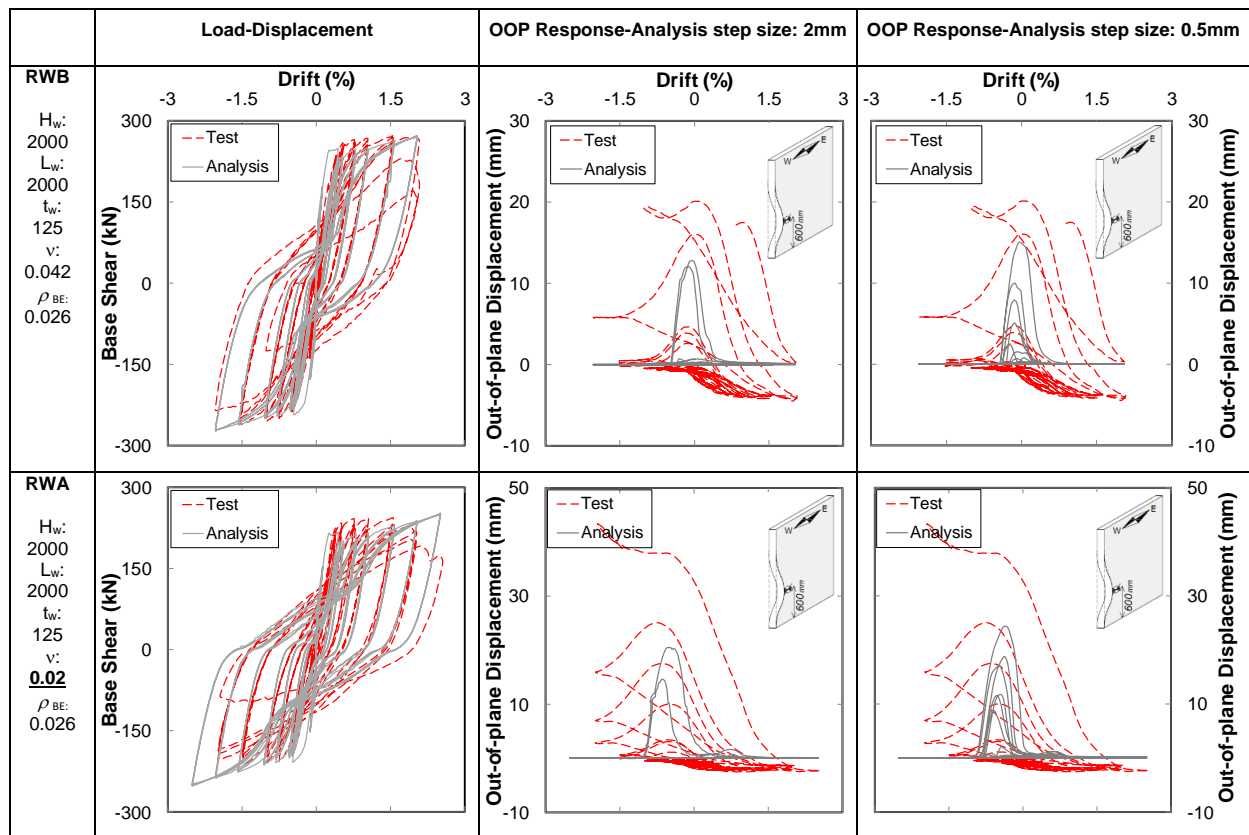


Fig. 6. Numerical prediction vs experimental measurements: Load-displacement and OOP-top displacement



## 5. Conclusions

An experimental study was conducted to investigate the effects of axial load on progression of OOP instability in structural walls. The test results are analysed in this paper and the salient features regarding the influence of axial load on the evolution of OOP deformation and subsequent instability in rectangular RC walls under in-plane cyclic loading are discussed. The main findings from this study are summarized below.

Axial load affects the level of strain developed in the longitudinal reinforcement at different stages of a loading cycle. Although its effect on the maximum tensile and compressive strains is negligible, the strain history between these two extremes is significantly controlled by the variation of axial load. At lower axial loads, the load-displacement curves are less pinched and crack closure of the cracked wall section during unloading/reloading stages occurs relatively late. The OOP deformation increases up to the crack closure on one face of the wall and thereafter the OOP deformation starts to recover until the crack closes fully on both faces of the wall. Therefore, the point in the drift history corresponding to the maximum OOP displacement depends on the level of axial load. With higher axial loads, this point would shift towards the beginning of reloading in the opposite direction and the OOP deformation could recover faster due to faster development of crack closure. The increase of axial load up to a certain level can increase the OOP displacement due to greater P-Delta effect, and its further increase would generate relatively pinched load-displacement curves. With the fast crack closure in such cases, the OOP displacement decreases and could recover fully if the axial loads are significantly high.

Depending on the stage of loading, the axial load ratio can have a mixed effect on the development of out-of-plane wall instability. Any level of compressive axial load can be beneficial in delaying the development of out-of-plane instability because the tensile strain in longitudinal reinforcement (key trigger for initiation of out-of-plane deformation) is decreased. Conversely, once the longitudinal reinforcement strain exceeds the critical tensile strain (i.e., tensile strain after which global out-of-plane eccentricity is generated), any magnitude of compressive axial load can become detrimental by generating a P-Delta moment that accelerates the out-of-plane deformation of the section. Therefore, the design provisions to avoid out-of-plane instability in structural walls cannot, therefore, be restricted to a specific range of axial load ratios.

## 6. Acknowledgements

The authors wish to acknowledge the financial support provided by the Building Systems Performance branch of the New Zealand Ministry of Business, Innovation and Employment (MBIE) and the Quake Centre at University of Canterbury to conduct this research.

## 7. References

- [1] Sritharan S, Beyer K, Henry RS, Chai Y, Kowalsky M and Bull D. (2014). "Understanding poor seismic performance of concrete walls and design implications". *Earthquake Spectra*, **30**(1): 307-334.
- [2] Oesterle R, Fiorato A, Johal L, Carpenter J, Russell H and Corley W. (1976). "Earthquake Resistant Structural Walls: Tests of Isolated Walls", PCA Serial No. Report 1571, Research and Development Construction Technology Laboratories, Portland Cement Association.
- [3] Goodsir WJ. (1985). "The design of coupled frame-wall structures for seismic actions", University of Canterbury. PhD.
- [4] Johnson B. (2010). "Anchorage detailing effects on lateral deformation components of R/C shear walls", Master Thesis, University of Minnesota.
- [5] Telleen K, Maffei J, Heintz J and Dragovich J. (2012a). "Practical Lessons for Concrete Wall Design, Based on Studies of the 2010 Chile Earthquake". 15th World Conference on Earthquake Engineering, 24-28 September 2012, Lisbon, Portugal.
- [6] Paulay T and Priestley M. (1993). "Stability of ductile structural walls". *ACI Structural Journal*, **90**(4): 385-392.



- [7] Chai YH and Elayer DT. (1999). "Lateral stability of reinforced concrete columns under axial reversed cyclic tension and compression". *ACI Structural Journal*, **96**(5): 780-789.
- [8] Dashti F, Dhakal RP and Pampanin S. (2014). "Simulation of out-of-plane instability in rectangular RC structural walls". Second European Conference on Earthquake Engineering and Seismology, Istanbul, Turkey.
- [9] Dashti F, Dhakal RP and Pampanin S. (2018). "Validation of a numerical model for prediction of out-of-plane instability in ductile structural walls under concentric in-plane cyclic loading". *Journal of structural engineering*, **144**(6): 04018039.
- [10] Menegon S, Wilson J, Gad E and Lam N. (2015). "Out-of-plane buckling of limited ductile reinforced concrete walls under cyclic loads". 2015 NZSEE Conference, Rotorua, New Zealand.
- [11] Rosso A, Almeida J and Beyer K. (2016). "Stability of thin reinforced concrete walls under cyclic loads: state-of-the-art and new experimental findings". *Bulletin of Earthquake Engineering*: 1-30.
- [12] Dashti F, Dhakal RP and Pampanin S. (2018). "Evolution of out-of-plane deformation and subsequent instability in rectangular RC walls under in-plane cyclic loading: Experimental observation". *Earthquake Engineering & Structural Dynamics*, **47**(15): 2944-2964.
- [13] Taleb R, Tani M and Kono S. (2016). "Performance of confined boundary regions of RC walls under cyclic reversal loadings". *Journal of Advanced Concrete Technology*, **14**(4): 108-124.
- [14] Rosso A, Jiménez-Roa LA, de Almeida JP, Zuniga APG, Blandón CA, Bonett RL and Beyer K. (2017). "Cyclic tensile-compressive tests on thin concrete boundary elements with a single layer of reinforcement prone to out-of-plane instability". *Bulletin of Earthquake Engineering*.
- [15] Haro AG, Kowalsky M, Chai Y and Lucier GW. (2018). "Boundary elements of special reinforced concrete walls tested under different loading paths". *Earthquake Spectra*, **34**(3): 1267-1288.
- [16] Tripathi M, Dhakal RP, Dashti F and Gokhale R. (2020). "Axial Response of Rectangular RC Prisms Representing the Boundary Elements of Ductile Concrete Walls". *Bulletin of Earthquake Engineering (under review)*.
- [17] Dashti F, Dhakal RP and Pampanin S. (2018). "Blind prediction of in-plane and out-of-plane responses for a thin singly reinforced concrete flanged wall specimen". *Bulletin of Earthquake Engineering*, **16**(1): 427-458.
- [18] Dashti F, Dhakal RP and Pampanin S. (2019). "A parametric study on out-of-plane instability of doubly reinforced structural walls. Part I: FEM predictions". *Bulletin of Earthquake Engineering (under review)*.
- [19] Dashti F, Tripathi M, Dhakal RP and Pampanin S. (2019). "A parametric study on out-of-plane instability of doubly reinforced structural walls. Part II: Experimental investigation". *Bulletin of Earthquake Engineering (under review)*.
- [20] NZS3101:2006. (2017). "Concrete Structures Standard, Parts 1&2 (Amendment No. 3)", Standards New Zealand.
- [21] NZS3101:2006. (2008). "Concrete Structures Standard, Parts 1&2 (Amendment No. 2)", Standards New Zealand.
- [22] Dashti F, Dhakal RP and Pampanin S. (2017). "Tests on slender ductile structural walls designed according to New Zealand standard ". *Bulletin of the New Zealand Society for Earthquake Engineering*, **50**(4): 504-516.
- [23] Dashti F. (2017). "Out-of-plane Instability of Rectangular Reinforced Concrete Walls Under In-plane Loading", PhD Thesis, Department of Civil and Natural Resources Engineering, University of Canterbury. PhD: 294.
- [24] Dashti F, Dhakal R and Pampanin S. (2018). "Local vs Global Instability of Ductile Structural Walls". 2018 NZSEE Conference, Auckland, New Zealand.
- [25] Dashti F, Dhakal R and Pampanin S. (2020). "Out-of-plane response of in-plane loaded ductile structural walls: State-of-the-art and classification of the observed mechanisms". *Journal of Earthquake Engineering*.
- [26] Dashti F, Dhakal RP and Pampanin S. (2018). "Inelastic Strain Gradients in Reinforced Concrete Structural Walls". 16th European Conference on Earthquake Engineering, Thessaloniki, Greece.
- [27] Dashti F, Dhakal RP and Pampanin S. (2017). "Numerical modeling of rectangular reinforced concrete structural walls". *Journal of Structural Engineering*, **143**(6): 04017031.